

Faint galaxy population in clusters: X-ray emission, cD halos and projection effects.

Carlos A. Valotto¹, Hernán Muriel¹, Ben Moore² and Diego G. Lambas¹
 val@oac.uncor.edu, hernan@oac.uncor.edu, ben.moore@durham.ac.uk, dgl@oac.uncor.edu

ABSTRACT

We analyze samples of nearby clusters taken from the Abell catalog and the X-ray Sample of Bright Clusters (De Grandi et al 1999) including a wide range of X-ray luminosities. Using the usually adopted background subtraction procedures, we find that galaxies in clusters selected by means of their X-ray emission show a flat luminosity function (faint end slope $\alpha \simeq -1.1$) consistent with that derived for galaxies in the field and groups. By contrast, the sample of Abell clusters that do not have an X-ray counterpart shows a galaxy luminosity function with a steep faint end ($\alpha \simeq -1.6$).

We investigate the possibility that cD halos could be formed by the disruption of galaxies in rich relaxed clusters that show an apparently flat faint end galaxy luminosity function (Lopez-Cruz et al 1997). We find that clusters dominated by a central cD galaxy (Bautz-Morgan classes I and II) show the same systematic trend: X-ray selected clusters have flatter faint end slopes than those clusters with no detected X-ray emission. Thus, it is likely the X-ray selection and not the cluster domination by central galaxies what correlates with background decontamination estimates of the galaxy luminosity function. Moreover, no significant correlation between X-ray luminosity and the galaxy LF faint end slope is found. These results do not support a scenario where flat faint end slopes are a consequence of cD formation via the disruption of faint galaxies. We argue that the clusters without X-ray emission are strongly affected by projection effects which give rise to spurious faint end slopes estimated using background subtraction procedures (Valotto et al 2001).

Subject headings: galaxies: luminosity function; galaxies: clusters; galaxies: X-Ray

¹IATE, Observatorio Astronómico, Laprida 854, Córdoba and CONICET, Argentina.

²Institute for Theoretical Physics, University of Zürich, Winterthurerstrasse 190, CH-8057 Zürich, Switzerland

1. Introduction

Determining the galaxy luminosity function (hereafter LF) down to faint magnitudes in rich clusters has been the subject of many studies in the last years (*e.g.* Sandage, Binggeli & Tammann 1985; Driver et al. 1994, De Propris et al. 1995; Lobo et al. 1997; Lumsden et al. 1997; Lopez-Cruz et al. 1997; Valotto et al. 1997; Wilson et al. 1997; Smith et al. 1997; Trentham 1998a; Trentham 1998b; Driver et al. 1998; Garilli et al. 1999). Most of these authors show that galaxy clusters are dominated by a large population of high surface brightness dwarf galaxies, corresponding to a steep faint end slope of the luminosity function, α in the range -1.4 to -2.0.

The origin and evolution of this faint galaxy population has important consequences for our current understanding of galaxy formation and evolution in dense environments. For instance, Lopez-Cruz et al (1997) have suggested that the galaxy LF is flat in dynamically evolved clusters characterized by the presence of a dominant cD galaxy, high richness, symmetrical single-peaked X-ray emission, and high gas mass. On the other hand, steep faint-end slopes ($-2.0 \leq \alpha \leq -1.4$) are detected in poorer clusters. It is worth noticing the fact that the galaxy luminosity function of groups selected in redshift space is flat at faint magnitudes (Muriel, Valotto & Lambas, 1998) which shows the lack of a universal trend of the parameter α with system richness. More recently, Martinez et al. (2002), have obtained reliable determinations of galaxy LF in groups obtained from the 2dF galaxy redshift survey. Their results are consistent with a nearly universal galaxy LF with little dependence on environment which is consistent with these previous findings. Lopez-Cruz et al. (1997) suggest that cD galaxies are formed from the disruption of many faint galaxies in the cluster cores, thus resulting in a globally flat faint end slope. Indeed, dynamical processes operating in relaxed clusters are, in general, destructive. Ram pressure stripping (Gunn & Gott 1972, Abadi, Moore & Bower 1999) and gravitational tides/galaxy harassment (*e.g.* Moore et al. 1996) both tend to fade galaxies by removing gas or stripping stars. These process are most effective for smaller, less bound galaxies, and would cause a flattening of the faint end slope. However, mergers and galaxy interactions, when the cluster environment then was more like a group environment could have contributed in the opposite direction at early evolutionary stages.

Although large deep redshift surveys of clusters are not presently available, Ferguson & Sandage (1991), and Zabludoff & Mulchaey (2000) have analyzed cluster fields with redshift information and obtained faint end slopes $\alpha \sim -1.25$ to -1.3 , which are not significantly steeper than field and group measurements in the 2dF galaxy redshift survey, Norberg et al. 2001, Martinez et al. (2002) both consistent with $\alpha \sim -1.13$. Most other estimates of galaxy luminosity functions in clusters rely critically on background subtraction and are

in general consistent with significantly steeper faint end slopes ($\alpha \leq -1.5$). The accuracy of this procedure depends on the statistical assumption that galaxy clusters correspond to density enhancements unbiased with respect to the distribution of foreground or background galaxies. However, significant projection effects are found in Abell clusters (e.g. Lucey 1983, Sutherland 1988, Frenk et al 1990) that can systematically bias the observed correlation function and the mass function of these systems. In fact, van Haarlem et al (1998) claim that one third of Abell clusters are not real physically bound systems but simply projections of galaxies and groups along the line of sight.

Valotto, Moore and Lambas (2001) have analyzed several sources of systematic effects present in observational determinations of the galaxy luminosity function in clusters. They used mock catalogues derived from numerical simulations of a hierarchical universe to identify clusters of galaxies in two dimensions in a similar fashion to Abell 1958 and Abell et al. 1989. Applying standard background subtraction procedures to these data gave rise to artificially steep faint end slopes since many of the clusters do not have significant counterparts in physical space. These projection effects result almost entirely from the large scale structure behind the cluster, a result that was also concluded by Adami et al (2000) from measuring ~ 100 redshifts for faint galaxies thought to lie in the Coma cluster. Color information (eg. $b-r$) is useful to improve the signal to noise in the process of background decontamination by efficiently removing red background galaxies at $z \geq 0.5$. However, very unlikely contaminating structures at significantly lower redshifts would be eliminated by the use of colors. See for instance Adami et al. (2000) where a significant number of background galaxies in the field of Coma Clusters are at $0.02 < z < 0.3$.

The X-ray emission of the hot intracluster gas provides a confirmation of the presence of a bound cluster of galaxies. Thus, estimates of the galaxy luminosity function in clusters by means of background decontamination techniques restricted to an X-ray selected sample may provide a useful insight on the issues previously mentioned. In this paper we explore the nature of the faint galaxy population in clusters obtained by background decontamination techniques in X-ray and optically identified clusters of galaxies. By considering a subsample restricted to clusters dominated by a central cD galaxy we can also explore the disruption hypothesis suggested by Lopez Cruz et al (1997).

2. Analysis

2.1. Cluster samples

The sample of galaxy clusters used in our statistical analysis is taken from Abell et al (1989) cluster catalog and from the X-ray flux-limited sample of Bright X-ray Clusters (De Grandi et al 1999, hereafter BXS), an X-ray selected cluster sample based on the first analysis of the ROSAT All-Sky Survey data (RASS1). This sample is count-rate limited in the ROSAT hard band (0.5-2.0 keV) and its effective flux limits varies between $\simeq 3$ and 4×10^{-12} ergs cm^{-2} s^{-1} .

The region explored is limited to galactic latitude $b < -40^\circ$ and declination $-70^\circ < \delta < -10^\circ$ and the area covered by the RASS1 Bright Sample. This survey area is restricted to regions with high exposure time ($> 150\text{s}$), excluding the sky areas of the Galactic plane and the Magellanic clouds to avoid incompleteness in the cluster sample. Due to the lack of homogeneity of the sky coverage of the ROSAT All-Sky Survey, we have checked the positions of those Abell clusters with no X-ray counterpart to eliminate from the statistics objects in the poorly sampled regions (see Figure 1).

In the area considered there are 34 Abell clusters and 15 X-ray clusters with redshift $z < 0.06$. Eight of these Abell clusters are identified with X-ray emission in this sample. Table 1 and table 2 list angular positions (J2000.0), mean redshifts, richness number counts and Bautz-Morgan types for the different samples analyzed here taken from Abell, Crown & Olowin 1989. A low redshift cutoff is required in order to reach faint absolutes magnitudes which unambiguously determine the α parameter.

2.2. LF Determination

The Edinburgh-Durham Southern Galaxy Catalog, hereafter COSMOS Survey (Heydon-Dumbleton et al 1989), was used for the statistical assignment of galaxies to the clusters. This survey provides angular positions and photographic magnitudes in the b_j band for over two million galaxies. We have restricted to the region $\delta < -10^\circ$ given the lower quality in the photographic material in the northern hemisphere. We use a limiting apparent magnitude, $b_j = 20.0$ (Valotto et al 1997), for our analysis of the COSMOS Survey which minimizes errors due to misclassification of stars, galaxies plate variations, etc. Incompleteness effects arise mainly due to star-galaxy misclassification. In the COSMOS survey the latter is expected to be lesser than 10% at $m=20.5$, and completeness to be greater than 99.5 % at $b_j=19.5$ (see Szapudi & Gaztañaga, 1998 for a comparison between COSMOS and APM survey statistical

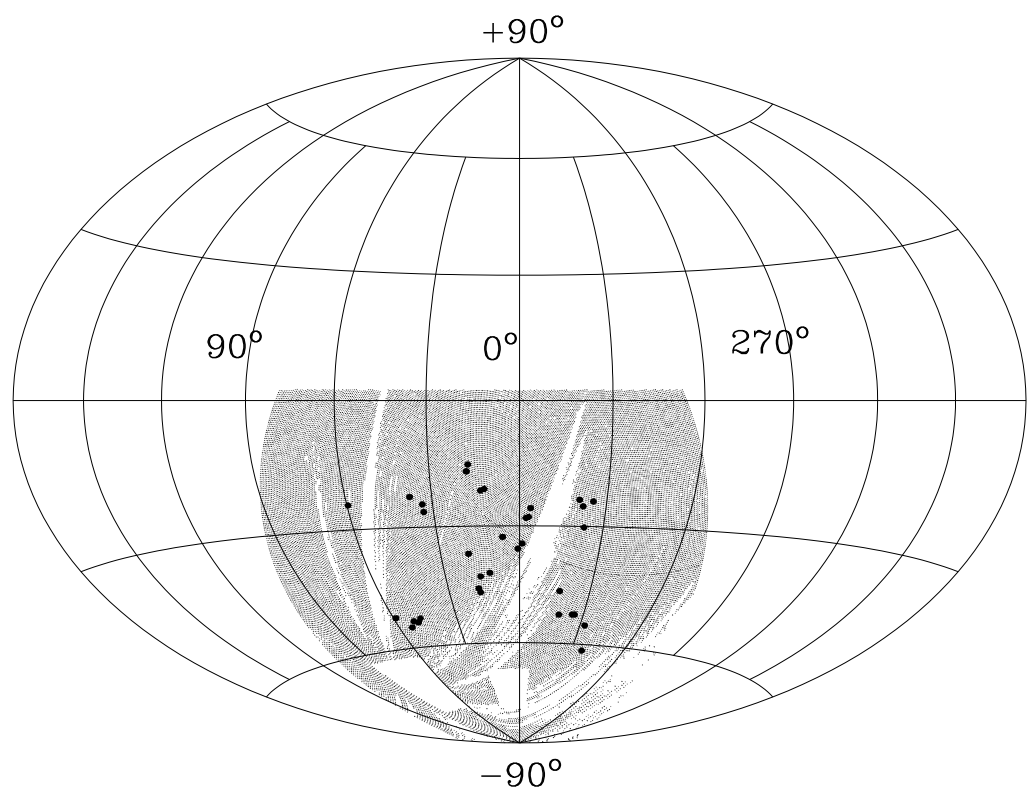


Fig. 1.— Projected distribution of Abell clusters and the area covered by the ROSAT Bright Sample in equatorial coordinates (De Grandi et al., 1999)

properties).

The counts of galaxies for each cluster are binned in equal number intervals. We subtract the corresponding mean background correction to each magnitude bin to compute the contribution from each cluster to the LF. We compute the number of galaxies brighter than a limiting absolute magnitude M_{lim} within a projected radial distance r from the cluster centers. The limiting absolute magnitude used is $M_{\text{lim}} = -16.5$. We have applied a K -correction term of the form $K = 3z$ (Efstathiou, Ellis & Peterson 1988). The projected radius r is fixed at $1.0 \text{ } h^{-1} \text{ Mpc}$. We assume the Hubble constant is $H_0 = 100 \text{ } h \text{ km s}^{-1} \text{ Mpc}^{-1}$, similar to that adopted in other studies. Since cluster redshifts are very small ($z \leq 0.06$) we simply use the local euclidean approximation.

We define a mean local background around each cluster in order to perform a statistical background subtraction. This mean local background is defined as the number density of galaxies in the same range of apparent magnitudes in a ring at projected radii $R_1 < r < R_2$. We have used $R_1 = 6 \text{ Mpc } h^{-1}$ and $R_2 = 8 \text{ Mpc } h^{-1}$.

According to Valotto et al. (1997) the stability of the results does not depend crucially on the projected clusters radii nor on the adopted radius for the background correction provided that the decontamination ring is well beyond the average projected radius of the clusters and small enough in order to take into account local variations of the projected galaxy density due to patchy galactic obscuration, large scale gradients in the galaxy catalog, etc.

For all samples we compute error bars in the galaxy LF through bootstrap resampling of the clusters to provide an estimate of the variations from cluster to cluster.

In order to provided suitable fits for the galaxy luminosity functions, we have adopted a Schechter function model $\phi(L)dL = C \times (L/L^*)^\alpha e^{-L/L^*} d(L/L^*)$, where C is a constant (Schechter 1977). We have applied a maximum likelihood estimator using the χ^2 -estimator procedure, which minimize the difference

$$\chi^2 = \sum_{i=1}^N \left[\frac{\phi_i - \phi(L_i; C, \alpha, L^*)}{\sigma_i} \right]^2,$$

where ϕ_i is the relative frequency of galaxies corresponding to the i th bin and σ_i is its associated uncertainty. All galaxy luminosity functions were arbitrarily normalized in order to make a proper comparison of their shapes.

3. Results

In this section we discuss the results obtained from the analysis of our cluster samples defined above. In Figure 2 we show the galaxy LF for the sample of bright X-ray clusters. For comparison we show the LF for the sample of Abell clusters in the same area of the sky and for the same range of redshifts. The solid lines correspond to Schechter function fits with parameters $\alpha = -0.9 \pm 0.1$, $M^* = -19.0 \pm 0.2$ and $\alpha = -1.50 \pm 0.1$, $M^* = -20.3 \pm 0.2$ for the X-ray and Abell samples respectively. The X-ray defined cluster sample has a significantly flatter faint end slope than the sample of Abell clusters.

We have also computed the galaxy LF for two subsamples of Abell clusters: those confirmed by the X-ray intracluster emission, and those with no X-ray detection. The results for these two samples are shown in Figure 3. Again we find a clear difference in the LF of clusters with and without X-ray emission. Abell clusters with no detected X-ray emission show a very steep galaxy LF faint end which contrasts with the flat behavior of the galaxy LF in X-ray confirmed clusters. The corresponding Schechter fits are $\alpha = -1.0 \pm 0.1$, $M^* = -18.9 \pm 0.2$ and $\alpha = -1.6 \pm 0.1$, $M^* = -20.6 \pm 0.2$ for the Abell clusters with and without X-ray detection respectively

A main point in the analysis of Lopez-Cruz et al (1997) is the suggestion that cD halos could be formed by accretion and disruption of galaxies resulting in a flattening of the faint end slope of the LF. Lopez-Cruz et al (1997) have suggested a scenario where the flat faint end of the galaxy LF in relaxed clusters results from the disruption of dwarf galaxies during the early stages of cluster evolution which also may explain the halos of central cD galaxies and a substantial fraction of the intracluster medium. We have tested this hypothesis by computing the galaxy LF for a subsample of clusters with Bautz-Morgan (BM) types I and I-II characterized by the presence of a dominant cD galaxy (this restricts our analysis to Abell clusters for which BM types are available). The first subsample corresponds to clusters selected in X-rays and the second subsample to clusters with no detection of X-ray emission. The results shown in Figure 4 suggests that the BM type of the clusters does not determine the faint end galaxy LF. Clusters with no detected X-ray emission have steep galaxy LF, on the contrary, clusters with detected X-ray emission show flat galaxy LF at the faint end.

The corresponding Schechter fits are $\alpha = -1.0 \pm 0.1$, $M^* = -19.1 \pm 0.1$ and $\alpha = 1.7 \pm 0.2$, $M^* = -20.2 \pm 0.2$ for the X-ray and non x-ray subsamples respectively. This test indicate that the detection of a faint population of faint galaxies is not correlated with dominant central galaxies but with the X-ray confirmation.

In Lopez-Cruz et al. 1997 scenario, it would also be expected that the slope of the faint end LF should correlate with the X-ray luminosity, i.e. the most luminous X-ray clusters

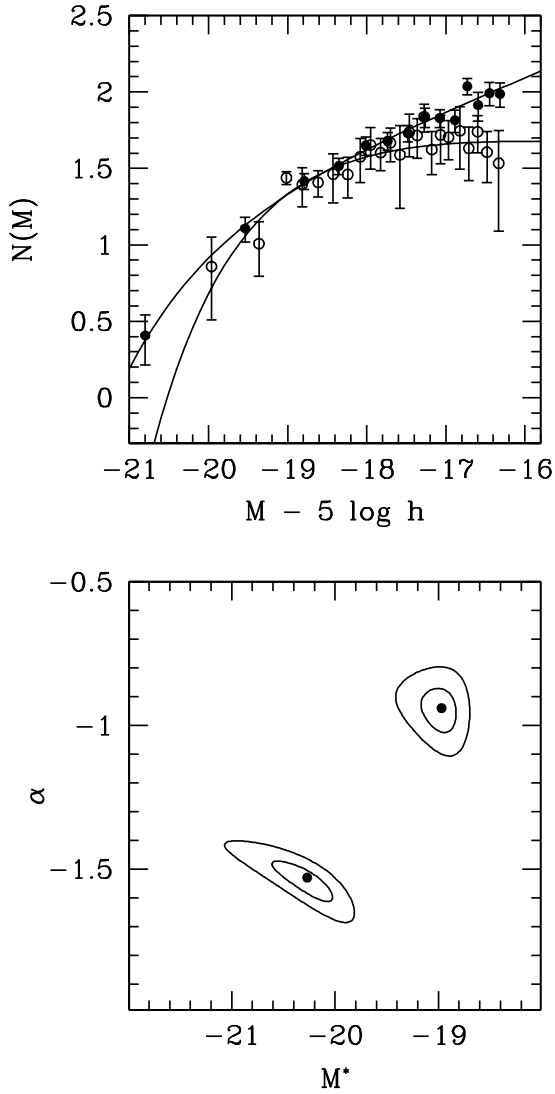


Fig. 2.— Galaxy luminosity function $N(M)$ for cluster galaxies of the Bright Cluster Sample (15 objects), open circles, and Abell clusters (35 objects), solid circles, corresponding to. The solid line shows the best Schechter function fits for these samples: $M^* = -19.0 \pm 0.1$, $\alpha = -0.9 \pm 0.1$ $M^* = -20.3 \pm 0.2$, $\alpha = -1.5 \pm 0.1$ respectively. The galaxy luminosity function is computed within a projected radial distance from the cluster center $r = 1.0$ Mpc h^{-1} . Error bars correspond to bootstrap resampling estimates.

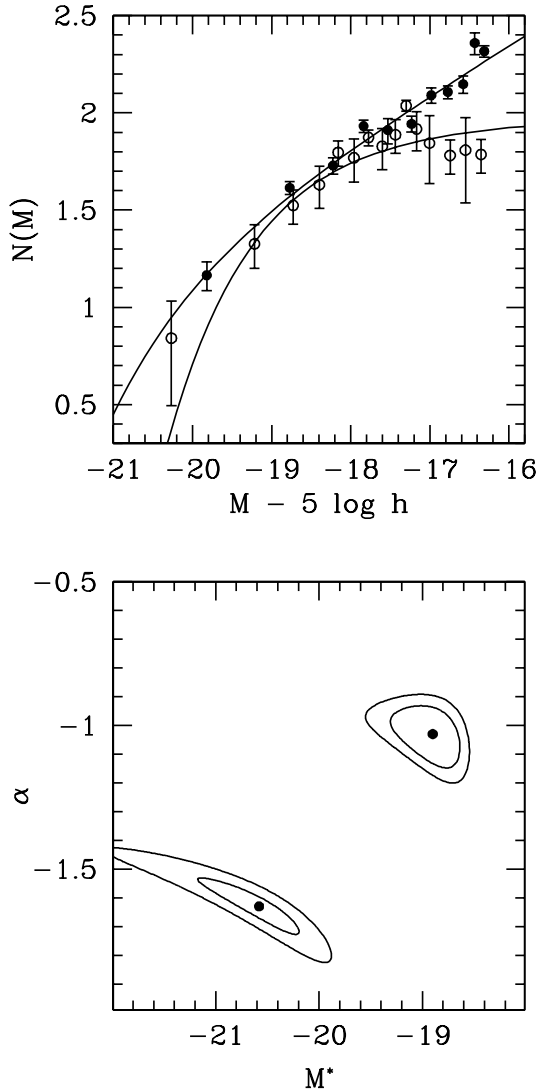


Fig. 3.— Galaxy luminosity function $N(M)$ for galaxies in clusters from the Bright Cluster Sample that are also within the Abell catalog (9 objects), open circles, and Abell clusters with no X-ray counterpart (20 objects), solid circles. The solid line shows the best Schechter function fits for these samples: $M^* = -18.9 \pm 0.2$, $\alpha = -1.0 \pm 0.1$ $M^* = -20.6 \pm 0.2$, $\alpha = -1.6 \pm 0.1$ respectively. The projected radial distance r and the error bars are the same as in figure 2.

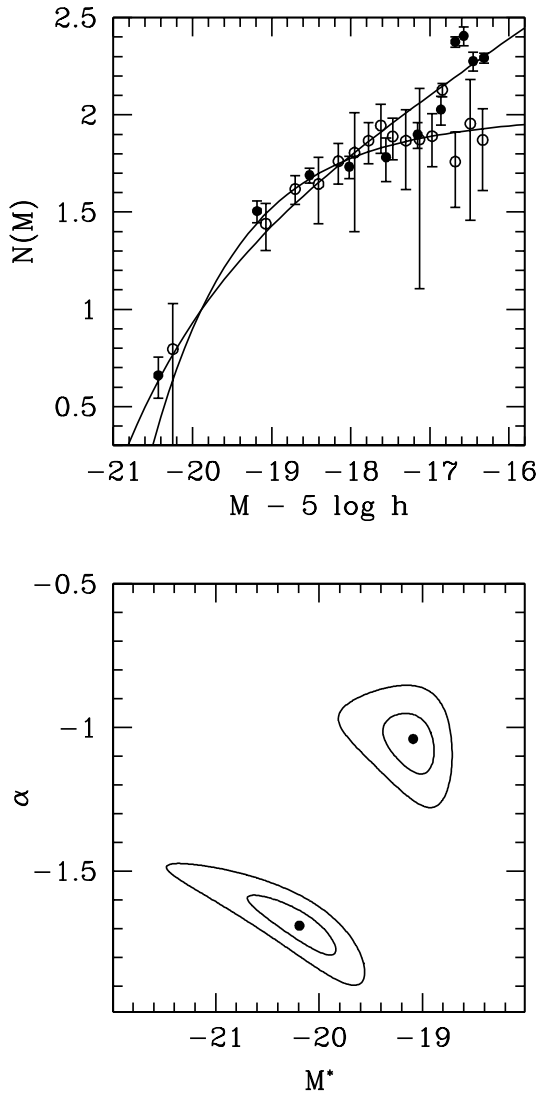


Fig. 4.— Galaxy luminosity function $N(M)$ for galaxies in clusters with Bautz-Morgan types I and I-II of the Bright Cluster Sample with Abell identification (6 objects), open circles, and Abell clusters with no X-ray counterpart (10 objects), solid circles. The solid line shows the best Schechter function fits for these samples: $M^* = -19.1 \pm 0.1$, $\alpha = -1.0 \pm 0.1$ $M^* = -20.2 \pm 0.2$, $\alpha = -1.7 \pm 0.1$ respectively. The projected radial distance r and the error bars are the same as in figure 2.

should have the flattest galaxy LF faint end slopes. We explore this possibility by dividing our X-ray cluster sample into equal numbers of clusters corresponding to high and low X-ray luminosity ($L_x > 1.0 \times 10^{44}$ ergs $\text{cm}^{-1} \text{s}^{-1}$ and $L_x < 1.0 \times 10^{44}$ ergs $\text{cm}^{-1} \text{s}^{-1}$) which correspond to mean luminosities of 2.44 and 0.83×10^{44} ergs $\text{cm}^{-1} \text{s}^{-1}$ respectively.

The resulting LF's are shown in Figure 5 and we find no differences between the two subsamples ($\alpha = -1.1 \pm 0.3$, $M^* = -18.6 \pm 0.2$ and $\alpha = -1.1 \pm 0.3$, $M^* = -18.8 \pm 0.2$ for low and high X-ray luminosity sample respectively), although the numbers of clusters in each sample is small. This result indicates that it is the detection of the intracluster medium through the X-ray emission and not its luminosity that correlates with the faint end slopes, giving support to the hypothesis of strong projection contamination in optically identified cluster samples.

We have analyzed samples of clusters which no dominant central galaxies, i.e. BM types II, II-III and III. We confirm here that, again, X-ray detectability and not the presence or absence of dominant central galaxies correlates with the α parameter obtained from background decontamination.

In order to test far a possible dependence of our results on cluster radii, we have analyzed all samples within two different limiting radii, $R = 0.5h^{-1}$ Mpc and $R = 1.0h^{-1}$ Mpc. We find similar results for these two samples which indicates a lack of strong radial dependence (see however de Propis et al. 1995).

Table 3 summarizes all of the parameters for the Schechter function fits to the various cluster subsamples. (We find no difference in our measurements of the faint end slope when we constrain the value of M^* to be the same value for each data set.)

We have also explored the ratio of dwarf to giant galaxies (D/G, D: $-18.5 < B_j < -16.5$, G: $-24 < B_j < -18.5$) in order to test the stability of our results when Schechter functions give poor fits to the actual LF. We have computed the D/G ratios for all samples analyzed and we show the results in table 3. As it can be seen by inspection to this table D/G and α are strongly correlated, all clusters with $\alpha > -1.2$ have $D/G < 4$ while samples with raising faint end slopes, $\alpha < -1.4$, have $D/G > 5$. Thus, D/G ratios provide confidence on our faint end slope estimates.

4. Discussion and Conclusions

We have analyzed the galaxy LF obtained by background decontamination techniques in samples of nearby clusters taken from Abell et al. 1989 and the Bright X-ray Cluster

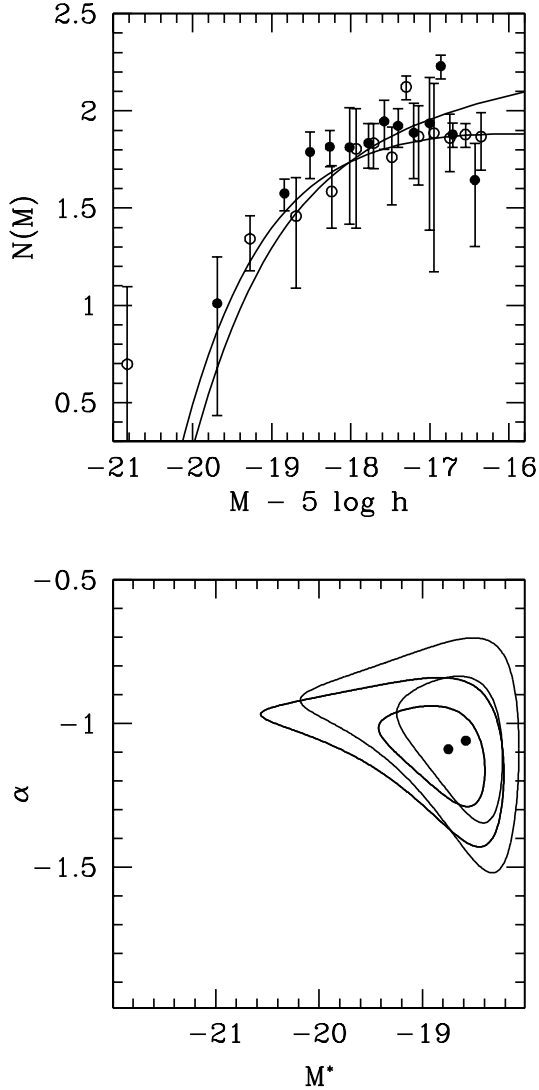


Fig. 5.— Galaxy luminosity function $N(M)$ for galaxies in clusters of the Bright Cluster Sample with low X-ray luminosity ($L_x < 1.0 \times 10^{44}$ ergs $\text{cm}^{-1} \text{s}^{-1}$, 4 objects), open circles, and high luminosity ($L_x > 1.0 \times 10^{44}$ ergs $\text{cm}^{-1} \text{s}^{-1}$, 5 objects), solid circles. The solid line shows the best Schechter function fits for these samples: $M^* = -18.8 \pm 0.3$, $\alpha = -1.1 \pm 0.2$ $M^* = -19.6 \pm 0.3$, $\alpha = -1.1 \pm 0.2$ respectively. The projected radial distance r and the error bars are the same as in figure 2.

Catalogues (De Grandi et al. 1999). We find that X-ray selected clusters show an apparently flat luminosity function consistent with that derived for the field and groups ($\alpha \simeq -1$). By contrast, clusters of galaxies identified from the projected galaxy distribution that do not have an X-ray counterpart show a galaxy luminosity function with a very significant steeper faint end ($\alpha \simeq -1.5$).

We find that for the subsample of clusters with dominant central galaxies (Bautz-Morgan type I and I-II) the shape of the faint end galaxy LF depends on the detection of the X-ray emission of the intracluster gas. In fact, we derive a steep galaxy LF for the subsample of clusters with central dominant galaxies with no detected X-ray intracluster emission. This fact argues against the hypothesis that the disruption of faint galaxies would provide the material out of which cD halos form causing a flattening of the faint end slope. A note of caution should be set here since we have used Bautz-Morgan classes as a suitable division between cD and non-cD clusters. Although some BM type I and I-II clusters may not contain bona fide cD galaxies, these clusters are strongly dominated by a central galaxy, so it is on the global, statistical sense that our analysis provide a test of Lopez-Cruz et al. hypothesis.

Our results could be influenced by the possibility that many X-ray undetected clusters could be bound systems less dynamically evolved and therefore with a large fraction of emission line galaxies which have a steeper alpha than non-emission line galaxies (Madgwick et al. 2002). Nevertheless, Martinez et al. 2002 have shown that even low mass groups ($M_{virial} \sim 10^{13} - 10^{14} M_{\odot}$) in the 2dF galaxy redshift survey are dominated by absorption line type galaxies suggesting that this is not a very serious possibility.

More likely, our results provide support to the presence of biases on the cluster galaxy LF derived by background decontamination procedures due to projection effects, as suggested by Valotto, Moore and Lambas (2001). Clusters identified from the projected galaxy distribution are biased by many spurious clumps with no physically bound system along the line of sight. The resulting luminosity functions from background decontamination procedures show steep faint end slopes and can be erroneously interpreted as the clusters being dominated by a population of dwarf galaxies. Furthermore, the fact that no significant correlation between X-ray luminosity and the galaxy LF faint end slope is found argues against processes associated to the gaseous environment causing the differences in the galaxy LF faint end slope.

5. Acknowledgments

We thank the anonymous Referee for very helpful suggestions which greatly improved the previous version of this paper. This research was supported by grants from Agencia Córdoba Ciencia, Secretaría de Ciencia y Técnica de la Universidad Nacional de Córdoba, Fundación Antorchas, and Agencia Nacional de Promoción Científica, Argentina. CV is supported by the National Science Foundation through grant #GF-1003-00 from the Association of Universities for Research in Astronomy, Inc., under NSF cooperative agreement AST-9613625.

REFERENCES

Abadi, M., Moore, B. & Bower, R., 1999, MNRAS, 308, 947.

Adami, C., Ulmer, M.P., Durret, F., Nichol, R.C., Mazure, A., Holden, B.P., Romer, A.K. & Savine, C. 2000, A&A, 353, 930.

Abell, G.O. 1958. ApJS, 3, 211.

Abell, G.O., Corwin, H.G & Olowin R.P. 1989, ApJ, 407, L49.

Cole, S., Hatton, S., Weinberg, D.H. & Frenk, C.S., 1998, MNRAS, 300, 945.

Cole, S., Aragón-Salamanca, A., Frenk, C.S., Navarro, J.F., Zepf, S., 1994, MNRAS, 271, 781.

De Grandi, S. et al., 1999, ApJ. 514, 148.

De Propris, R., Pritchett, C.J., Harris, W.E. & McClure, R.E., 1995, ApJ, 450, 534.

Driver, S.P., Phillipps, S., Davies, J.I., Morgan, I., Disney, M.J. 1994, MNRAS, 268, 393.

Driver, S.P., Couch, W.J., Phillipps, S., Smith, R., 1998, MNRAS, 301, 357.

Driver, S.P., Couch, W.J., Phillipps, S., 1998, MNRAS, 301, 369.

Efstathiou, G., Ellis, R.S. & Peterson, B.A. 1988, MNRAS, 232, 431.

Ferguson, H.C. & Sandage, A., 1991, AJ, 101, 765.

Frenk, C.S., White, S.D.M., Efstathiou, G., Davis, M., 1990, ApJ, 351, 10.

Kauffmann, G., White, S.D.M., Guiderdoni, B. 1993, MNRAS, 264, 201.

Gaidos, E.J., A.J., 113, 117.

Garilli, B., Maccagni, D., Andreon, S., 1999, A&A. 342, 408.

Heydon-Dumbleton, N.H. Collins. C.A.,& MacGillivray, H.T., 1989, MNRAS, 238, 379.

Lobo, C., Biviano, A., Durret, F., Gerbal, D., Le Fevre, O., Mazure, A., Slezak, E. 1997, AA, 317, 385.

Lopez-Cruz, O., Yee, H.K.C., Brown, J.P., Jones, C., Forman, W., ApJ, 475, 97.

Lumsden, S.L., Nichol, R.C., Collins, C.A., Guzzo, L. 1992, MNRAS, 258, 1.

Lumsden, S.L., Collins, C.A., Nichol, R.C., Eke, V.R. & Guzzo, L., 1997, MNRAS, 290, 119.

Maddox, S.J., Efstathiou, G., Sutherland, W.J., Loveday, J., 1990a, MNRAS, 243, 692.

Maddox, S.J., Efstathiou, G., Sutherland, W.J., 1990b, MNRAS, 246, 433.

Madgwick, D.S et al., 2002, MNRAS, 336, 907.

Mateo, M, 1998, Annu. Rev. Astron. Astrophys., 36, 435.

Moore, B., Katz, N., Lake, G., Dressler, A., Oemler, A., 1996, Nature, 379, 613

Muriel, H., Valotto, C.A. & Lambas, D.G., 1998, ApJ, 290, 119.

Loveday, J., Peterson, B.A., Efstathiou, G. & Maddox, S.J., 1992, MNRAS, 390, 338.

Sandage, P., Binggeli, B. & Tammann, G.A., 1985, MNRAS, 90, 1795.

Smith, R.M., Driver, S.P., Phillipps, S. 1997, MNRAS, 287, 415.

Sutherland, W.J., 1988, MNRAS 234, 159.

Schechter, P., 1976, ApJ, 203, 197.

Szapudi, I. & Gaztañaga, E., 1998, MNRAS, 300, 493.

Trentham, N., 1998, MNRAS, 294, 193.

Trentham, N., 1998, MNRAS, 286, 133.

Valotto, C.A., Nicotra, M.A., Muriel, H. & Lambas, D.G., 1997, ApJ, 479, 90.

Valotto, C.A., Moore, B. & Lambas, D.G., 2000, ApJ, 546, 157.

van Haarlem, M., Frenk, C.S. & White, S.D.M., 1997, MNRAS, 287, 817

Wilson, G., Smail, I., Ellis, R.S., Couch, W.J, 1997, MNRAS, 284, 915.

Zabludoff, A.I. & Mulchaey, J.S., 2000, ApJ, 539, 136.

Zucca E. et al. 1997, A&A, 326, 477.

Table 1. Sample of Abell Clusters with no X-ray identification

Name	α	δ	z	<i>AbellRichness</i>	<i>BM</i>
A2731	00 10.2	-56 59	0.0312	39	III
A2806	00 40.2	-56 09	0.0275	37	I-II
A2824	00 48.6	-21 20	0.0486	46	III
A0114	00 53.7	-21 40	0.0580	43	-
A2870	01 07.7	-46 54	0.0250	33	I
A2877	01 09.8	-45 54	0.0231	30	I
A2881	01 11.2	-17 04	0.0445	36	II
A2882	01 11.4	-17 04	0.0455	32	II
A2896	01 18.3	-37 06	0.0317	44	I
A2933	01 40.7	-54 33	0.0208	77	III
A2992	02 14.9	-26 40	0.0584	30	I
A2995	02 15.2	-24 50	0.0370	69	I-II
A0419	03 08.5	-11 31	0.0410	32	-
A3093	03 10.9	-47 23	0.0635	93	I
A3125	03 27.4	-53 30	0.0590	46	III
A3144	03 37.1	-55 01	0.0430	54	I-II
A3193	03 58.2	-52 20	0.0345	41	I
A3816	21 50.3	-55 17	0.0389	39	I-II
A3782	21 34.5	-62 01	0.0557	40	II
A3851	22 16.7	-52 35	0.0520	33	I-II
A3869	22 21.4	-52 34	0.0396	49	II
A3893	22 38.0	-23 54	0.0330	39	I
A3925	22 51.8	-46 35	0.0510	38	II
A4012	23 31.8	-33 49	0.0510	35	II-III
A4013	23 31.9	-35 16	0.0500	51	III
A2660	23 45.3	-25 58	0.0520	45	-

Table 2. Bright X-ray Cluster subsample

Name	α	δ	z	<i>Abell Richness</i>	BM	$L_x[10^{44}erg s^{-1}]$
A4038	23 47.7	-28 08	0.0290	117	III	1.01
A4059	23 56.7	-34 40	0.0470	66	I	1.79
A3911	22 46.1	-52 43	0.0381	58	II-III	2.43
A3880	22 27.8	-30 34	0.0581	31	II	0.90
A3158	03 42.9	-53 38	0.0591	85	I-II	3.36
A0133	01 02.6	-21 47	0.0604	47	-	2.16
A0151	01 08.9	-15 25	0.0536	72	II	0.77
A2717	00 03.3	-35 57	0.0498	52	I-II	0.64
S0041	00 25.6	-33 03	0.0566			0.68
0118.5-1408	01 21.0	-13 51	0.0511			1.03
S0301	02 49.6	-31 11	0.0223			0.10
1ES0412-382	04 14.0	-38 06	0.0502			0.84
ESO235-G050	21 04.8	-51 49	0.0491			0.88
ESO146-G028	22 29.0	-60 54	0.0412			0.24
S1101	23 14.0	-42 44	0.0580			1.93

Table 3. Results

Sample Description	Number of cluster	α	M^*	D/G
Abell	34	-1.5 ± 0.1	-20.3 ± 0.2	5.45 ± 0.16
BXS	15	-0.9 ± 0.1	-19.0 ± 0.1	3.20 ± 0.16
Abell non-X	26	-1.6 ± 0.1	-20.6 ± 0.2	6.46 ± 0.22
Abell X	8	-1.0 ± 0.1	-18.9 ± 0.2	3.94 ± 0.25
Abell I, I-II non-X	12	-1.7 ± 0.1	-20.2 ± 0.2	5.74 ± 0.31
Abell I, I-II X	3	-1.0 ± 0.1	-19.1 ± 0.1	3.87 ± 0.26
BXS, low X	4	-1.1 ± 0.2	-18.8 ± 0.3	3.34 ± 0.30
BXS, high X	4	-1.1 ± 0.2	-18.6 ± 0.3	3.84 ± 0.42